

## **EXPERIMENTALLY ASSESSING THE PERFORMANCE OF AN ABSORPTION CHILLER TO CALIBRATE A MODEL OF A THERMALLY ACTIVATED CHILLER**

Geoff Johnson, Ian Beausoleil-Morrison

School of Mechanical and Aerospace Engineering, Carleton University, Ottawa, Canada

### **ABSTRACT**

Solar cooling is an alternative to conventional electrically driven vapour compression technology that could result in environmental benefits and a reduced demand upon the central electrical grid during system-wide peak periods. Currently solar cooling technology is in an early market state and it is unclear whether or not these systems can meet performance demands. Literature indicates that the benefits of solar cooling are largely dependent on geography. To investigate the viability of solar cooling in Canada, a thermally activated absorption chiller has been installed in a laboratory and a test bench has been designed and developed. The performance of this device is currently being measured under controlled operating conditions. The measured performance data is intended to be used to calibrate an existing absorption chiller model in ESP-r. Once calibrated, the absorption chiller model may be used to simulate how solar cooling will perform in Canadian environments.

### **INTRODUCTION**

The dominant technology for residential space cooling in Canada is electrically driven vapour compression systems. Conventional vapour compression air conditioners draw a large amount of power from the central electrical grid during the summer months when cooling loads are highest; particularly in the late afternoon and early evening. Air conditioning power draw during these periods of peak consumption is often supplied by burning greenhouse gas intensive fuels that contribute to climate change. As the population grows and the climate becomes warmer, the number of conventional air conditioners in use is increasing. Solar driven thermally activated cooling is gaining attention as an alternative to conventional systems since solar energy is most available during the cooling season.

In a solar air conditioning system, solar thermal collectors gather the sun's energy to heat water. Hot water produced from the solar thermal collectors is used to activate a thermal cooling cycle. Thermodynamic cycles that are suitable for solar cooling applications can be characterized as being

hydraulically activated at temperatures of 80°C to 100°C; the water temperature produced by most solar thermal collectors. Mugnier (2006) reports that of all the operating solar cooling systems 63% use absorption 8% use adsorption and 29% use desiccant cooling cycles. Because the use of the absorption cycle in solar air conditioning applications is currently the most widespread it will be the focus of this research.

The useful cooling effect in a closed cooling cycle is produced by the evaporation of a refrigerant at a cold temperature in the evaporator. In a conventional vapour-compression refrigeration cycle, the refrigerant vapor from the evaporator is compressed using mechanical work to a higher pressure level. The compressor of a conventional vapor compression air-conditioning unit is replaced by a generator, absorber and pump in the absorption cycle.

Little research on solar thermally activated cooling has been published in Canada. There has only been one recent study performed in North America: Davanagere, Sherif, and Goswami (1999) investigate the performance of a solid desiccant cooling system using numerical simulation for four cities in the United States: Jaxsonville, Albuquerque, New York, and Houston. The lack of Canadian research in the field of solar air conditioning is the motivation for this research.

### **EXPERIMENTAL APPARATUS**

To evaluate the feasibility of solar cooling technology for residential applications in Canada, a Yazaki WFC-SC10 lithium/bromide absorption chiller has been purchased by Carleton University. Currently the chiller is being commissioned in a laboratory test facility to assess the chiller's performance under varying and controlled operating conditions.

It is well known that the temperatures of the fluid streams which feed the absorption chiller influence the coefficient of performance directly. In practice, weather, solar collector characteristics, storage medium and system control affect the temperature of the water delivered to the condenser, absorber,

evaporator and generator so it is important to understand the performance of a chiller under a variety of operating conditions for solar cooling applications. The purpose of the test facility is to characterize the performance of the chiller for a range of heat medium, chilled and cooling water temperatures and flow rates.

A schematic of the test facility is illustrated in Figure 1. An electrical in-line heater will mimic the building's cooling load and will be modulated to control the evaporator inlet temperature. A second electrical in-line heater will mimic the solar collector heat source and will be modulated to control the generator inlet temperature. PID controllers execute the control algorithm to maintain set water temperatures to the inlets of the chiller. Thermocouples will be installed with thermopiles to provide controllers with the input necessary to control water temperatures and for data acquisition with Labview.

A cooling tower will not be employed as a heat sink. Outlet cooling water from the chiller will instead exchange heat with a cold water stream supplied by other building chillers for re-cooling. A proportioning valve controlled by Labview will maintain a set cooling water temperature to the chiller inlet. The outlet cooling water and chilled water streams pass through a heat exchanger to decrease the cooling burden on the heat sink.

The amount of cooling water that exchanges heat with the chilled water is controlled by a manual valve. Fixed speed pumps circulate the fluid in all circuits. Flow control is achieved using balance valves at chiller inlets in all fluid circuits. Stop valves are employed at chiller outlets to isolate the chiller from the fluid circuits when the chiller must be removed from the test bed. Table 1 indicates the experimental quantities of interest and how they will be measured.

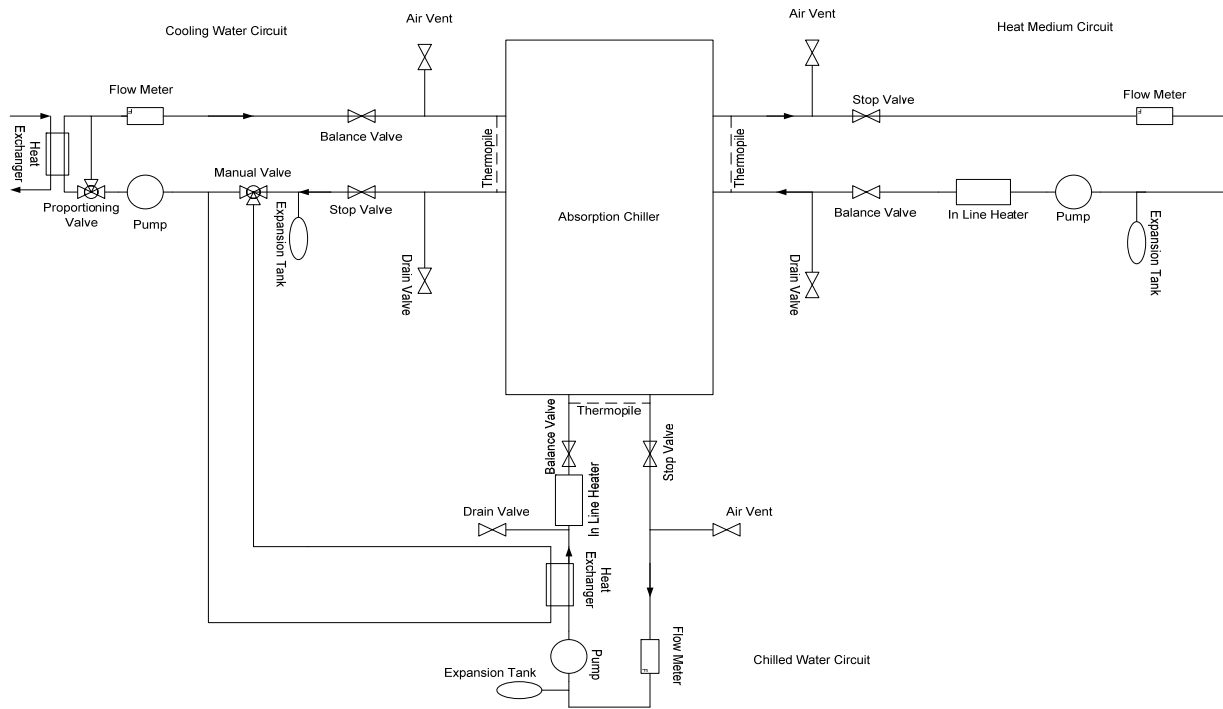


**Figure 1: Carleton University absorption chiller test bed apparatus**

| Measured Quantity | Instrument          | Description                          |
|-------------------|---------------------|--------------------------------------|
| $T_{GI}$          | Type T Thermocouple | Generator Inlet Temperature          |
| $T_{GO}$          | Type T Thermocouple | Generator Outlet Temperature         |
| $\Delta T_G$      | Type T Thermopile   | Generator Temperature Difference     |
| $\dot{m}_G$       | Oval Gear Flowmeter | Generator Mass Flow Rate             |
| $T_{EI}$          | Type T Thermocouple | Evaporator Inlet Temperature         |
| $T_{EO}$          | Type T Thermocouple | Evaporator Outlet Temperature        |
| $\Delta T_E$      | Type T Thermopile   | Evaporator Temperature Difference    |
| $\dot{m}_E$       | Oval Gear Flowmeter | Evaporator Mass Flow Rate            |
| $T_{CI}$          | Type T Thermocouple | Cooling Water Inlet Temperature      |
| $T_{CO}$          | Type T Thermocouple | Cooling Water Outlet Temperature     |
| $\Delta T_C$      | Type T Thermopile   | Cooling Water Temperature Difference |

**Table 1: experimentally measured quantities**

The chiller requires thermal input from three externally pumped fluid circuits: a heat medium (HM), chilled (CH) and cooling (C) water circuit. Table 2 lists the chiller's requirements from the three external circuits.

| Circuit | Temperature (°C) | Flow Rate (L/min) |
|---------|------------------|-------------------|
| HM      | 80-95            | 49-170            |
| CH      | 7-20             | 72-110            |
| C       | 23-33            | 306-356           |

**Table 2: fluid circuit requirements**

The flow rates in Table 2 were met in the test assembly by using the pumps listed in the following table. Note that the flow rate for the chilled water circuit was met by operating two pumps in parallel.

| Circuit | Pump      | Power (kW) |
|---------|-----------|------------|
| HM      | CR 10-3   | 2.24       |
| CH      | CR 3-5    | 0.56       |
| C       | SSV32 1/1 | 3.73       |

**Table 3: external pumps**

The temperature ranges required by the chiller were met by using electric in-line heaters. The heaters are listed in the following table. Note the heating requirement of the heat medium circuit necessitated the use of two electric in-line heaters operating in series. Each heater is operated by a control box containing PID controllers. Labview is used to operate the controller.

| Circuit | Heater                | Capacity (kW) |
|---------|-----------------------|---------------|
| HM      | CRES-ILB-48-0300-K-3P | 30            |
| HM      | CRES-IBL-48-0250-K-3P | 25            |
| CH      | CRES-ILB-48-0300-K-3P | 30            |

**Table 4: electric in-line heaters**

The schematic in Figure 1 calls for two heat exchangers in the external fluid circuits. A M110-30 brazed plate heat exchanger operates with a manual bypass valve between the chilled and cooling water circuit. A M110-70 brazed plate heat exchanger operates between the cooling water and an externally chilled line. The external chilled water line provides a flow of 98 L/min at 7°C.

The heat exchangers have been sized to exchange the loads listed in the following table. Flow conditions used for sizing were in the range listed in Table 2.

| Heat Exchanger | Capacity (kW) |
|----------------|---------------|
| M110-30        | 35            |
| M110-70        | 70            |

**Table 5: heat exchanger performance**

A controlled proportioning valve modulates the cooling water chiller inlet temperature using Labview. The valve controls the amount of water bypassing the heat exchanger with the externally chilled stream. The valve is a 2", three way mixing valve. The valve actuator has a control time of 60s.

### ESP-R ABSORPTION CHILLER MODEL

Building simulation is a useful tool that may be used to assess the feasibility of solar cooling for different climate regions. An existing simulation model of an

absorption chiller in ESP-r has been developed and was described by Beausoleil-Morrison (2004).

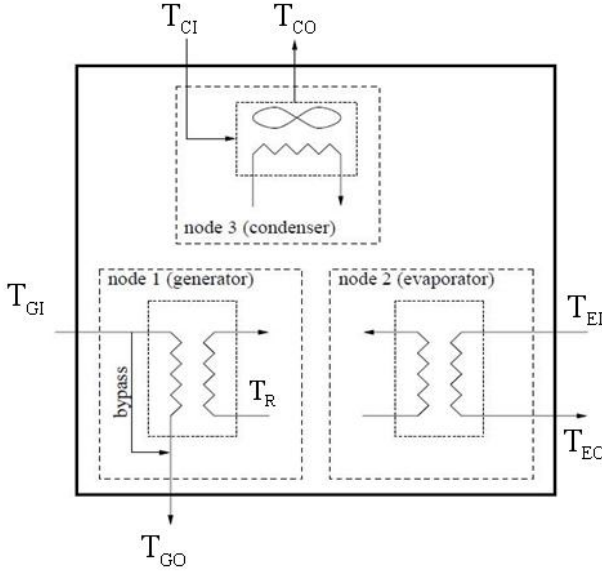


**Figure 2: ESP-r absorption chiller model Ref: Beausoleil-Morrison, 2004**

The model illustrated in Figure 2 depicts the current ESP-r absorption chiller model. The absorption chiller model consists of three nodes. Each node consists of two fluid streams which come into thermal contact in a heat exchanger. This model does not explicitly model the thermodynamics of an absorption chiller and instead relies on experimental calibration.

The generator and evaporator equations follow. The expressions are derived by using the first law of thermodynamics. It is assumed in this analysis that the nodes have no heat capacity other than that of the fluid streams.

$$T_{GO} = T_{GI} - \frac{\dot{q}_G}{(\dot{m}c_p)_G}$$

$$T_{EO} - COP \cdot \frac{(\dot{m}c_p)_G}{(\dot{m}c_p)_E} \cdot T_{GO} - T_{EI} = -COP \cdot \frac{(\dot{m}c_p)_G}{(\dot{m}c_p)_E} \cdot T_{GI}$$

$\dot{q}_G$  in the above equations represents the heat transferred across the generator heat exchanger which is used to drive the cycle.  $c_p$  represents the heat capacity of water, assumed to be constant.

The condenser node equation may be found by a similar analysis to that conducted for the evaporator and generator. The expression for the condenser node is given as follows.

$$T_{CO} + \frac{(\dot{m}c_p)_G}{(\dot{m}c_p)_C} \cdot T_{GO} + \frac{(\dot{m}c_p)_E}{(\dot{m}c_p)_C} \cdot T_{EO} = \frac{\dot{q}_{pump}}{(\dot{m}c_p)_C} + T_{amb} + \Delta_{Cond} + \frac{(\dot{m}c_p)_G}{(\dot{m}c_p)_C} \cdot T_{GI} + \frac{(\dot{m}c_p)_E}{(\dot{m}c_p)_C} \cdot T_{EI}$$

In the the above equation  $\dot{q}_{pump}$  represents heat gains from the pump used to circulate solution inside the absorption chiller.

The condenser inlet temperature is given by the the following equation.

$$T_{CI} = T_{amb} + \Delta_{Cond}$$

$T_{amb}$  represents the outdoor dry bulb temperature; it is determined from weather files.  $\Delta_{Cond}$  represents local heating effects to the condenser inlet; it is a user controlled parameter.

The preceding equations were intended to be complemented with a thermal coefficient of performance ( $COP$ ) function that was to be determined experimentally along with a generator capacity " $\dot{q}_G$ ". Beausoleil-Morrison (2009) indicated that a lack of experimental data describing the dependence of chiller thermal  $COP$  on chiller water circuit temperatures currently results in simplifications to solar cooling system models and is a limitation.

The goal of this research is to produce data that can be used to create  $COP$  and  $\dot{q}_G$  functions for the absorption chiller model. It is expected the functions shall depend on the following variables.

$$\dot{q}_G = f(T_{GI}, T_{EI}, T_{CI}, \dot{m}_G, \dot{m}_E)$$

$$COP = \frac{\dot{q}_E}{\dot{q}_G} = f(T_{GI}, T_{EI}, T_{CI}, \dot{m}_G, \dot{m}_E)$$

## DATA ANALYSIS

The data gathered will be used to compute a derived thermal COP which follows.

$$COP = \frac{(\dot{m}c_p \Delta T)_E}{(\dot{m}c_p \Delta T)_G}$$

The experimental uncertainty of the derived COP can be calculated by considering the bias and anticipated precision errors of the individual measurements using the standard ASME measurement uncertainty methods outlined by Moffat (1988).

For a derived quantity “ $r$ ” that depends on some other parameters “ $P_i$ ”:

$$r = f(P_1, P_2, \dots, P_i)$$

The sensitivity factors “ $\theta_i$ ” are found by:

$$\theta_i = \frac{dr}{dP_i}$$

For COP the sensitivity factors are:

$$\frac{dCOP}{d\Delta T_E} = \frac{(\dot{m}c_p)_E}{(\dot{m}c_p \Delta T)_G}$$

$$\frac{dCOP}{d\dot{m}_E} = \frac{(c_p \Delta T)_E}{(\dot{m}c_p \Delta T)_G}$$

$$\frac{dCOP}{d\Delta T_G} = -\frac{(\dot{m}c_p \Delta T)_E}{(\dot{m}c_p \Delta T^2)_G}$$

$$\frac{dCOP}{d\dot{m}_G} = -\frac{(\dot{m}c_p \Delta T)_E}{(\dot{m}^2 c_p \Delta T)_G}$$

For  $\dot{q}_G$  the sensitivity factors are:

$$\frac{d\dot{q}_G}{d\Delta T_G} = (\dot{m}c_p)_G$$

$$\frac{d\dot{q}_G}{d\dot{m}_G} = (c_p \Delta T)_G$$

The overall bias “ $B$ ” and precision error “ $S$ ” of the derived quantity may be found from the individual measurements’ bias “ $B_i$ ” and precision errors “ $S_i$ ” by:

$$B = \sqrt{\sum (\theta_i B_i)^2}$$

$$S = \sqrt{\sum (\theta_i S_i)^2}$$

The overall 95% uncertainty level of the derived quantity “ $U$ ” may be found by combining the overall and bias and precision errors by:

$$U = \sqrt{tS^2 + B^2}$$

The following is an uncertainty analysis of the COP at published nominal operating conditions with known bias errors and anticipated precision errors.

| Parameter    | $P_i$     | $B_i$ ( $\pm\%$ ) | $S_i$ ( $\pm\%$ ) |
|--------------|-----------|-------------------|-------------------|
| $\Delta T_G$ | 5°C       | 2.2               | 2.2               |
| $\dot{m}_G$  | 2.4 kg/s  | 1.0               | 1.0               |
| $\Delta T_E$ | 4.7°C     | 2.2               | 2.2               |
| $\dot{m}_E$  | 1.53 kg/s | 1.0               | 1.0               |

**Table 6: parameter nominal operating condition value, known bias and expected precision**

The thermopile bias error listed in the preceding table was achieved by calibration. The calibration system components are listed in the following table along with their individual bias errors. Note that a five junction thermopile was needed to achieve the listed data acquisition system uncertainty of 2%.

| Component                 | Quantity | $B_i$ ( $\pm\%$ ) |
|---------------------------|----------|-------------------|
| Constant Temperature Bath | 2        | .3                |
| Reference Thermometer     | 2        | .6                |
| Data Acquisition System   | 1        | 2                 |

**Table 7: thermopile calibration system component bias errors**

Individual component biases may be combined into an overall system bias by the root mean square method given by the following equation. The result of combining the component biases is what is listed as the thermopile bias in Table 6.

$$B = \sqrt{\sum B_i^2}$$

The preceding error analysis using the values listed in Table 6 yields:

$$COP = 0.6 \pm 0.02$$

$$\dot{q}_G = 50 \pm 2 \text{ kW}$$

This demonstrates that the  $COP$  and  $\dot{q}_G$  may be determined experimentally by the proposed methods with acceptable uncertainty levels. Note that water density and specific heats have been assumed to be known with no uncertainty in this analysis. Specific heat of water was assumed to be 4.186 J/KgK.

Although the chiller test facility has been commissioned data has yet to be gathered. To gather data experiments will be performed in which different steady state inlet conditions will be supplied to the chiller while  $COP$  and  $\dot{q}_G$  are monitored. It is expected that four experiments per day should be feasible. The performance parameters likely depend upon five variables (listed below).

$$COP = \frac{\dot{q}_E}{\dot{q}_G} = f(T_{GI}, T_{EI}, T_{CI}, \dot{m}_G, \dot{m}_E)$$

$$\dot{q}_G = f(T_{GI}, T_{EI}, T_{CI}, \dot{m}_G, \dot{m}_E)$$

It should be possible to collect data in which the variable ranges listed in Table 2 are spanned by three data points each in a time period of approximately two months.

The gathered data will appear in a table such as the one listed below.

| $T_{EI}$ | $T_{GI}$ | $T_{CI}$ | $\dot{m}_G$ | $\dot{m}_E$ | $COP$ | $\dot{q}_G$ |
|----------|----------|----------|-------------|-------------|-------|-------------|
|          |          |          |             |             |       |             |
|          |          |          |             |             |       |             |

**Table 8: data table template**

For building simulation  $COP$  and  $\dot{q}_G$  function domains will be discretized. During an ESP-r simulation a  $COP$  and  $\dot{q}_G$  function value will be assigned to any arbitrary inlet condition based on the inlet condition that most closely matches in Table 8.

## CONCLUDING REMARKS

Current vapour compression air conditioning systems draw large amounts of electrical power (often during system-wide peak periods) and can be a significant burden on the central electrical grid during the cooling season. Solar cooling could be an alternative to conventional vapour compression systems which could potentially contribute to space cooling demands and benefit the environment. Literature indicates that solar cooling technology is currently in an early market state and research is ongoing to assess whether solar cooling systems can meet performance demands. Local geography and climate conditions have been identified as important factors contributing to system performance. Many studies which simulate and/or experimentally determine solar cooling system performance have been conducted however no studies have been performed that consider a Canadian environment. In order to begin to assess the feasibility of solar cooling in Canada a Yazaki solar thermal absorption chiller has been purchased and installed in a test facility at Carleton University. This article outlined the design and operation of the test facility and described how the measured data will be used to calibrate simulation models.

## ACKNOWLEDGEMENT

The authors are grateful for the funding provided by the Natural Sciences and Engineering Research Council of Canada through the Solar Buildings Research Network and through Ian Beausoleil-Morrison's Discovery Grant.

## REFERENCES

- Beausoleil-Morrison I. (2009). *On predicting the magnitude and temporal variation of cooling loads in detached residential buildings*. Carleton University
- Beausoleil-Morrison I. (2004). The simulation of a residential space-cooling system powered by the thermal output of a cogeneration device. *E-Sim*
- Davanagere B., Sherif S., Goswami D. (1999). A Feasibility study of a solar desiccant air-conditioning system-part II. *Transient Simulation and Economics, International Journal of Energy Research* 23, 103-116
- Henning H. (2007). *Solar Assisted Air-Conditioning in Buildings*. Springer Wien

Herold K. Radermacher R., Klein S. (1996)  
*Absorption Chillers and Heat Pumps*, CRC

Hidalgo M., Aumente P., Millan M., Neumann A., Mangual R. (2008). Energy and carbon emission savings in Spanish housing air-conditioning using solar driven absorption system. *Applied Thermal Engineering* 28, 1734-1744

Moffat R. (1988). Describing the Uncertainty in Experimental Results. *Experimental Thermal and Fluid Science* 1, 3-17

Mugnier D. (2006) Thermally driven water chillers: Market status and new developments, *IEA Task 38 – Solar air conditioning and refrigeration*